Redox Biology 52 (2022) 102295

Contents lists available at ScienceDirect

Redox Biology

journal homepage: www.elsevier.com/locate/redox

UCHL1 protects against ischemic heart injury via activating HIF-1α signal pathway

Bingchuan Geng [a], Xiaoliang Wang [a], Ki Ho Park [a], Kyung Eun Lee [a], Jongsoo Kim [a], Peng Chen [a], Xinyu Zhou [a], Tao Tan [a], Chunlin Yang [a], Xunchang Zou [b], Paul M. Janssen [c], Lei Cao [b], Lei Ye [d], Xuejun Wang [e], Chuanxi Cai [a], Hua Zhu [a,*]

[a] Department of Surgery, The Ohio State University Wexner Medical Center, Columbus, OH, 43210, USA
[b] Department of Cancer Biology and Genetics, The Ohio State University Wexner Medical Center, Columbus, OH, 43210, USA
[c] Department of Physiology and Cell Biology, Davis Heart and Lung Research Institute, The Ohio State University Wexner Medical Center, Columbus, OH, 43210, USA
[d] Department of Biomedical Engineering, School of Medicine and School of Engineering, University of Alabama at Birmingham, Birmingham, AL, 35233, USA
[e] Division of Basic Biomedical Sciences, University of South Dakota Sanford School of Medicine, Vermillion, SD, 57069, USA

ARTICLE INFO

Keywords:
UCHL1
Ischemic cardiac injury
HIF-1α
Deubiquitylating enzyme

ABSTRACT

Ubiquitin carboxyl-terminal esterase L1 (UCHL1) has been thought to be a neuron specific protein and shown to play critical roles in Parkinson's Disease and stroke via de-ubiquiting and stabilizing key pathological proteins, such as α-synuclein. In the present study, we found that UCHL1 was significantly increased in both mouse and human cardiomyocytes following myocardial infarction (MI). When LDN-57444, a pharmacological inhibitor of UCHL1, was used to treat mice subjected to MI surgery, we found that administration of LDN-57444 compromised cardiac function when compared with vehicle treated hearts, suggesting a potential protective role of UCHL1 in response to MI. When UCHL1 was knockout by CRISPR/Cas 9 gene editing technique in human induced pluripotent stem cells (hiPSCs), we found that cardiomyocytes derived from *UCHL1−/−* hiPSCs were more susceptible to hypoxia/re-oxygenation induced injury as compared to wild type cardiomyocytes. To study the potential targets of UCHL1, a BioID based proximity labeling approach followed by mass spectrum analysis was performed. The result suggested that UCHL1 could bind to and stabilize HIF-1α following MI. Indeed, expression of HIF-1α was lower in *UCHL1−/−* cells as determined by Western blotting and HIF-1α target genes were also suppressed in *UCHL1−/−* cells as quantified by real time RT-PCR. Recombinant UCHL1 (rUCHL1) protein was purified by E. Coli fermentation and intraperitoneally (I.P.) delivered to mice. We found that administration of rUCHL1 could significantly preserve cardiac function following MI as compared to control group. Finally, adeno associated virus mediated cardiac specific UCHL1 delivery (AAV9-cTNT-m-UCHL1) was performed in neonatal mice. UCHL1 overexpressing hearts were more resistant to MI injury as compare to the hearts infected with control virus. In summary, our data revealed a novel protective role of UCHL1 on MI via stabilizing HIF-1α and promoting HIF-1α signaling.

1. Introduction

The incidence of cardiovascular disease (CVD) is increasing every year. To date, CVD has become the leading cause of death in the western world. Myocardial infarction (MI) is a major disease in cardiovascular deaths [1,2]. Although morbidity is decreasing as a result of improving treatments after MI, long term effects of MI often result in heart failure (HF). Myocardial ischemia is the leading cause of the death of cardiomyocytes and eventual HF [3]. Hypoxia-inducible factor 1 (HIF-1) is a major regulator and transcriptional factor of the hypoxic response after MI [4]. It's a critical oxygen-sensitive transcription factor that orchestrates the body's protective responses to ischemia through transcriptional activation of up to 200 genes, which are essential for cell survival, and may therefore be important in the adaptation of the heart to tolerate ischemic injury [5].HIF-1 consists of two basic-helix-loop-helix/PAS transcription factors, HIF-1α and HIF-1β [6]. HIF-1α is sensitive to hypoxia and is rapidly degraded by the ubiquitin proteasomal pathway under normoxic condition [7]. Interestingly,

* Corresponding author. Department of Surgery, The Ohio State University Wexner Medical Center, 460 W 12th Ave., Columbus, OH, 43210, USA.
E-mail address: Hua.Zhu@osumc.edu (H. Zhu).

https://doi.org/10.1016/j.redox.2022.102295
Received 2 February 2022; Received in revised form 7 March 2022; Accepted 16 March 2022
Available online 18 March 2022

HIF-1α mainly expresses in myocardium, suggesting its potential role in myocardial development and protection [8]. Indeed, myocardial specific overexpression of HIF-1α protects against MI induced cardiac injury and maintained cardiac functions [9].

The ubiquitin proteasome system (UPS) is a fundamental regulator of protein quality control in all cells, including the cardiomyocyte, which participates in protein trafficking, cellular signal transduction, and prominently in degradation [10,11]. When components of the UPS function normally, the integrity of proteins that make up the sarcomere, mitochondria and cell membrane is maintained, allowing for normal heart function. Conversely, cardiac dysfunction is prominently associated with alterations in UPS function [12].

UCHL1, a crucial member of the deubiquitination protein family, is a multifunctional protein, which can control cell proliferation, differentiation, and cell damage by regulating the ubiquitination or non-ubiquitination pathways [13,14]. Our previous study demonstrated that UCHL1 promotes invasion of breast cancer cells [15]. Recent studies have demonstrated that inhibition of UCHL1 significantly ameliorated cardiac hypertrophy induced by agonist or pressure overload [16]. Other researchers found UCHL1 might promote post MI cardiac fibrotic remodeling in cardiac fibroblasts [17]. However, the role of UCHL1 in myocardial injury and repair has not been studied. In the current study, we found that UCHL1 significantly overexpressed in infarct and boarder zones of the hearts following MI. A novel *in vitro* proximity-dependent biotin labeling method was used to identify HIF-1α as the partner of UCHL1 following ischemic injury. In summary, our data suggested that.

2. Materials and methods

2.1. Cell culture

Urine derived human iPSC was purchased from Cellapy Biological (Beijing, China). iPSC line was cultured on Matrigel-coated plates (Corning REF.356231) using StemFlex medium (Thermo Fisher Cat. No. A3349401) under conditions of 37 °C, 95% air, and 5% CO2 in a humidified incubator. HEK293T cell line was cultured in an atmosphere of 37 °C, 95% air, and 5% CO2 in Dulbecco's modified Eagle's medium (DMEM) supplemented with 10% fetal bovine serum, 100 U/ml penicillin and 100 μg/ml streptomycin (all Sigma-Aldrich, Buchs, Switzerland).

2.2. Animal models

All animals were purchased from Jackson Laboratory. Animal surgery was performed at the University Laboratory Animal Resources of The Ohio State University in compliance with the National Institutes of Health Guide for Care and Use of Experimental Animals. Both male and female mice were used in this study. Mice were aged to eight weeks, at which point they underwent baseline echocardiography and followed by coronary artery ligation surgery. Briefly, mice were anesthetized and ventilated prior to open thoracotomy through the 4th rib followed by opening of the pericardium and left anterior descending (LAD) ligation with 10–0 suture. All surviving mice were subjected to follow-up echocardiography at different time points after surgery. Heart and other tissue were isolated from these mice for further analysis. Isoproterenol (Sigma-Aldrich, Buchs, Switzerland) is used for inducing heart failure in mice. Briefly, eight week old mice were subcutaneous injected with isoproterenol 150 mg/kg/day for one week. Three weeks later, echocardiography was used to confirm the success of isoproterenol induced heart failure and heart samples were isolated from these mice for further analysis.

2.3. Western blot analysis

Total protein was extracted from cells or tissue using a protein lysis buffer containing protease inhibitors (Roche Life Science, IN, USA). The denatured proteins were ran onto 12% SDS/polyacrylamide gels and the separated proteins were transferred to PVDF membranes (Merck Millipore, Berlin, Germany). Membranes are stained with Ponceau S solution (Sigma.P7170) and images were taken by Bio-Rad imaging system to show equal protein loading for each sample. Membranes were further probed with primary antibody and incubate at 4 °C over night. Then, they were washed with PBST and probed with secondary antibody. Protein expression is detected by Bio-Rad imaging system using chemiluminescent substrate (Thermo #34080). Antibodies used were as follows: UCHL1 (CST#13179), Hif-1α (GeneTex #GTX127309) , GAPDH (CST #5174 S), Ubiquitin (sc-8017).

2.4. Immunoprecipitation assay

Wild type and *UCHL1−/−* iPSC derived cardiomyocytes (iPSC-CM) were subjected to hypoxia treatment with or without 10 μM MG132. Three hours after hypoxia treatment, cells were washed with cold PBS and immediately lysed with lysis buffer. Cell lysis were immunoprecipitated with Hif-1α antibody (GeneTex #GTX127309) using the Immunoprecipitation Kit Dynabeads Protein G (Life Technologies) according to the manufacturer's instructions. Western blotting was performed using the indicated antibody.

2.5. Immunofluorescent staining

Cells are washed using PBS and fixed by using 4% paraformaldehyde for 15 min at room temperature. Fixed cells were permeabilized by 0.1% Triton X-100 for 20 min at room temperature followed by washing with PBS twice. Cells were blocked with 10% donkey or goat serum (the species where the secondary antibodies are raised) for 1 h and then incubated with primary antibodies diluted in blocking buffer plus 0.05% Tween-20 (PBST) at 4 °C overnight. Cells were subsequently thoroughly washed by PBST three times and then incubated with secondary antibodies conjugated with fluorescent dyes for 1 h at room temperature, followed by PBST wash for three times. Then the stained cells were treated with mounting media containing DAPI (Fluoromount-G, SouthernBiotech,cat.0100–20), and sealed by coverslips. Heart tissue sections were either from paraffin embedded heart samples or cryo blocks. Immunofluorescence staining were performed with antibodies against UCHL1 , Hif-1α and α-sarcomeric actin. Staining slides were visualized by either a Zeiss confocal microscope (LSM780) or a Leica thunder model organism imaging system. Antibodies used were as follows: UCHL1(CST#13179), Hif-1α (Novus #NB100-105) , monoclonal *Anti*-α-Sarcomeric Actin antibody (Sigma #A2172), Anti-rabbit IgG Alexa Fluor546 (A10040, Invitrogen), Anti-rabbit IgG Alexa Fluor647 (A21244, Invitrogen), Anti-mouse IgM Alexa Fluor 647 (A21238, Invitrogen), Anti-mouse IgM Alexa Fluor 555 (A21426, Invitrogen), Anti-mouse IgG Alexa Fluor 488 (A11029, Invitrogen). Use of human samples from control and patients with heart failure were approved by the Institutional Review Board (IRB) of The Ohio State University (study number 2012H0197). All participants in these studies provided written informed consent.

2.6. RNA extraction and real-time PCR

RNA was extracted from cells or mouse heart tissues by the Trizol method (Invitrogen, Carlsbad, CA), and 1 μg RNA was reverse transcribed by kit from Thermo(#K1691). Real-time reverse transcription

polymerase chain reaction (real time RT-PCR) was conducted with PerfeCTa SYBR Green FastMix (Quanta-bio, #95072–250). Primers for this study are as follows:

gene		Sequence (5′-3′)
Mouse GAPDH	forward	AACTTTGGCATTGTGGAAGG
	reverse	ACACATTGGGGGTAGGAACA
Mouse UCHL1	forward	CCCCGAAGATAGAGCCAAG
	reverse	ATGGTTCACTGGAAAGGG
Human ACTB	forward	CACCATTGGCAATGAGCGGTTC
	reverse	AGGTCTTTGCGGATGTCCACGT
Human UCHL1	forward	CTTCATGAAGCAGACCATTG
	reverse	ATCATGGGCTGCCTGTATG
Human CD39	forward	GCCCTGGTCTTCAGTGTATTAG
	reverse	CTTGATGCCACCACGTAAGA
Human LDHA	forward	GCCTGTGCCATCAGTATCTT
	reverse	ACCTCTTTCCACTGTTCCTTATC
Human VEGF-α	forward	GGAAGAGGAGGAGATGAGAGA
	reverse	CTCAGAAGCAGGTGAGAGTAAG
Human PDK1	forward	GTGCTCAGCCTCTCTGTAAAT
	reverse	GCCACCACTGAAGGTATCTATG
Human BNIP3	forward	GTTCCAGCCTCGGTTTCTATT
	reverse	CCGACTTGACCAATCCCATATC

2.7. Picrosirius Red staining

Picrosirius red staining was conducted with a kit from Polysciences company (#24901–250). Deparaffinize sections and hydrate to dH_2O. Place slides in Solution A for 2 min followed by rinsing in dH_2O. Place slides in Solution B for 60 min. Then place slides in Solution C for 2 min followed by 70% Ethanol for 45 s. Finally dehydrate, clear and mount slides.

2.8. Generation of UCHL1 knockout human induced pluripotent stem cells (hiPSCs)

A single clone of UCHL1−/− hiPSCs line was generated by CRISPR/Cas 9 genome editing method in our previous study [18]. Briefly, guide RNA (gRNA) was designing from website (crisprscan.org) to target exon3. The design are as follows: gRNA2: 5′-CACCGGCAGGT GCTGTCCCGGCTGG-3'; 5′- AAACCCAGCCGGGACAGCACCTGCC -3'. Oligos were heated and cooled down by a thermocycler for complementary annealing. Double-strand oligos were ligated into PX459V2.0-eSpCas9(1.1) plasmid (Addgene,#108292) linearized by *Bbs*I restriction enzyme (NEB, #R0539S). 4×10^5 human iPSCs were cultured in a 6-well plate for 3 days to reach a confluent of 80%. At day 3, 5 μg of constructed crispr vector and 0.5 μg of GFP plasmids (CRIPSR: GFP vector = 10:1) are co-transfected to 1×10^6 human iPSCs using neon system with the condition of 1200 V, 30 ms, 1 pulse. After electroporation 16hrs, change to selection culture medium with 10 μg/ml of puromycin (life technologies REF.A11138-03). After 24hrs of selection, change to normal medium and keep culturing for 4 days. Sterile cloning disks (Scienceware cat.#F37847-0001) are used to pick single iPSC clone. IPSCs are culturing in 48 well plate for one week then transfer to 6 well plate for further analysis. Stable knock-out cell lines were confirmed with Western blot and Sanger sequencing of genomic DNA.

2.9. hiPSCs cardiac differentiation

Cardiac differentiation of hiPSCs was initiated by using a small-molecule–mediated protocol [19]. Briefly, hiPSCs (passage 20–35) were cultured to 80–90% confluence and StemFlex media was replaced with cardiac differentiation basal media (RPMI + B27 supplement minus insulin) supplemented with 9 μM CHIR-99021 (Selleckchem). The medium was then changed with cardiac differentiation basal medium plus 5 μM of IWR-1 (Sigma). Differentiated cells were maintained in a cardiac differentiation basal medium for 2 days and substituted with a cardiac proliferation medium (RPMI + B27 supplement) for another 4 days. Beating hiPSC-CMs were typically observed on days 8–12 of differentiation. Beating hiPSC-CMs were then subjected to a glucose-free RPMI medium (Thermo Fisher Scientific) plus B27 supplement for 4 days for metabolic purification. The purified hiPSC-CMs were then passaged and replated in Matrigel-coated plates in a normal cardiac proliferation media (RPMI + B27 supplement).

2.10. Split-BioID analysis

pcDNA3.1 mycBioID plasmid was obtained from Addgene (#35700). UCHL1 sequence was obtained by PCR from Flag-HA-UCHL1 plasmid (Addgene # 181134). PCR primers are designed as follows: UCHL1-F; 5′-AAAAAGGATCCATGGAGATCAACCCCGAGATG-3'; UCHL1-R; 5′-AAA AACTCGAGTTAGGCTGCCTTGCAGAGAGC-3'. Double-strand PCR products were ligated into pcDNA3.1 mycBioID plasmid linearized by XhoI and BamHI restriction enzyme (NEB, #R0146S, #R0136S). UCHL1-BirA plasmid was transfected into HEK293T cell line. Transfected cells were changed medium with biotin (Sigma) followed by physical hypoxia (1% O_2, 5% CO_2, 94% N_2) and chemical hypoxia ($CoCl_2$). The protein was extracted followed by incubating with streptavidin magnetic beads (Thermo, #65001) at 4 °C overnight. The biotinated protein (UCHL1 interaction protein) was precipitated. Then the protein samples were subjected to electrophoretic separation by polyacrylamide gel electrophoresis and Western blot analysis.

2.11. Recombinant human UCHL1 purification

Human UCHL1 DNA sequence was subcloned into the pET28a vector (EMD Biosciences, Billerica, MA) with T4 DNA ligase (NEB, Ipswich, MA) to generate pET28a-rhUCHL1 plasmid. The pET28a-rhUCHL1 plasmid (with 6 his-Tag) was transformed into competent *E coli* strain BL21 (DE3) cells (Invitrogen). Then, *E coli* were incubated at 37 °C in Luria-Bertani medium with shaking (250 rpm). Isopropyl-β-D-thiogalactopyranoside (Amresco, Solo, OH) was added at a concentration of 1 mM when the OD_{600} of the *E coli* culture reached 0.4. After further incubation at 4 °C for 16 h, cells were harvested for further use. Rapid screening of expression cultures was performed according to the manual for high-level expression and purification of 6xHis-tagged proteins (Qiagen, Germantown, MD). ~ 24.8 kDa rhUCHL1 protein was purified and afterward it was verified by SDS-PAGE analysis. The purified His-rhUCHL1 protein was further confirmed by Western blot of anti-UCHL1 antibody. The purified protein was stored at −80°C freezer for further use.

2.12. UCHL1 AAV generation

Adeno-associated virus of AAV9-cTNT-m-Uchl1-WPRE (#AAV-275559) were prepared by Vector Biolabs. Expression of mouse UCHL1 gene is driven by cTNT promoter to ensure cardiomyocyte specific expression. Virus aliquots were stored at −80 °C and thawed before use. Murine experiments were conducted using wild-type C57BL/6J mice purchased from the Jackson Laboratory. Neonatal mice (2 or 3 day old) were used for UCHL1 delivery. Mice were placed in a container with crushed ice for ~1 min until the hypothermal anesthesia could take effect. Intravascular injection of virus were performed via superior temporal vein. A total of 50 μl of AAV9-cTNT-m-Uchl1-WPRE virus or same amount of control virus at 2×10^{11} GC with 2.5% Evans blue dye (Sigma-Aldrich, St. Louis, MO) was loaded into a syringe with 30-gauge needle. Following canalization of the vein, the virus solution was slowly injected. Since Evans blue dye was added into virus solution, successful injection will turn mouse to blue color immediately. After injection, neonatal mice were placed on a heating pad for recovery before being returned to their mother. Injected mice were subjected to MI surgery at 8 week old. Successful cardiac UCHL1 expression after virus neonatal superior temporal vein injection were confirmed with Western blotting.

2.13. Cell fractionation

Cells grown in 6-well dishes were washed wtih ice-cold PBS and collected into 1.5 ml micro-centrifuge tubes. Supernatants were removed from each sample and cell pellets were resuspended in 90 μl of ice-cold 0.1% NP40 (Sigma) in PBS and triturated 5 times. Thirty μl of the lysate was removed as whole cell lysate. The remaining material was centrifuged for 10 s and 30 μl of supernatant was removed as the cytosolic fraction. After the remaining supernatant was removed, the pellet was resuspended in 200 μl of ice-cold 0.1% PBS and centrifuged for 10 s and the supernatant was discarded. The pellet was resuspended with 30 μl of 1x Laemmli sample buffer and designated as nuclear fraction. Nuclear fractions and whole cell lysates that contained DNA were sonicated using microprobes.

2.14. Statistical analysis

A Student's t-test was used to determine statistical difference between groups.

3. Result

3.1. UCHL1 is upregulated in both human heart failure samples and murine myocardial infarction model

We first collected cryo-sections of failing human hearts (n = 11) and healthy control (n = 9). Immunostaining of UCHL1 was performed and quantified (Fig. 1A , B). We found UCHL1 was significantly upregulated in failing human hearts as compared to that in control ($p < 0.05$). Furthermore, the expression of UCHL1 is mainly in cardiomyocytes as marked by α-sarcomeric actin (Fig. 1A). To further study the dynamic expression of UCHL1, a mouse model of myocardial infarction (MI) was used. As shown in Fig. 1C, the expression of UCHL1 protein was very low in both the heart subjected to sham surgery and remote zone (uninjured) of hearts after MI surgery. Consistent to observation of human hearts, UCHL1 protein was significantly upregulated in infarct area of heart, starting at day 4 after surgery and remaining high through whole observation period (42 day) (Fig. 1C , D , F). Similar trend of upregulation of UCHL1 mRNA was also observed with real time RT-PCR analysis of heart tissues (Fig. 1E). Again, immunofluorescent staining showed that UCHL1 appeared at the border and infarct zones after MI surgery and was mainly expressed in cardiomyocytes (Fig. 1G and Supplemental Fig. S1). Furthermore, we have also analyzed the RNA sequencing data from our published study with porcine MI model [20]. We found that UCHL1 significantly increased in both infarct zone and border zone of MI animal hearts as compared that in anterior left ventricular wall of sham animals (Supplemental Fig. S2.), while UCHL3 and UCHL5 remained similar among different samples. Together, these results revealed UCHL1 upregulated in myocardium after MI injury in human hearts and multiple animal models, suggesting UCHL1 might play a role in cardiac injury and repair.

3.2. Pharmacological inhibition of UCHL1 compromises cardiac function following MI

To study the role of UCHL1 in cardiac injury, LDN57444, a UCHL1 small molecule inhibitor, was applied to treat the mice after MI surgery (Fig. 2A). Echocardiogram analysis showed the ejection fraction of the inhibitor treated group was significantly lower than that of the control group (Fig. 2B , 2C). Cardiac fibrosis was also demonstrated with Picrosirius Red staining. While there was a trend of higher fibrosis in the inhibitor treated group, there was no statistically difference between two groups (Fig. 2D , E). Taken together, these results suggested that inhibition of UCHL1 after MI compromises cardiac pumping function. The primary target of UCHL1 might be cardiomyocytes rather than cardiac fibroblasts.

3.3. HIF-1α is a potential target of UCHL1 after myocardial infarction

In order to identify the potential target of UCHL1 in myocardial infarction, we established a proximity-labeling system [15]. This system uses BirA, a ligase that biotinylates nearby proteins within an estimated proximity of 10 nm. By conjugating UCHL1 with BirA, we can label the proteins come to proximity to UCHL1 (Fig. 3A). We overexpressed BirA-UCHL1 in HEK293 cells and subjected them in physical (1% O2, 5% CO2, 94% N2) and chemical (0.5 mM $CoCl_2$) hypoxia. After running Western blotting analysis with pull down samples, Hif-1α was identified in the BirA-UCHL1 over-expression pull-down lysate (Fig. 3B). Our results are consistent with previous observations in cancer cells [21–23], which suggested the role of UCHL1 in deubiquitining and stabilizing HIF-1α. To further study the function of UCHL1 in regulating HIF-1α. We used established *UCHL−/−* hiPSCs and their wild type control [18]. We first differentiated hiPSCs into beating cardiomyocytes (hiPSC-CM). Then hiPSC-CM was transferred into hypoxia condition for 3, 6, and 12 h. As shown in Fig. 3C and **D**, while HIF-1α was observed after hypoxia, the upregulation of HIF-1α in wild type hiPSC-CMs was significantly higher than that in *UCHL1−/−* hiPSC-CM. More interestingly, expression of UCHL1 was also upregulated upon hypoxia treatment (Fig. 3E), which correlated well with HIF-1α upregulation. Then we performed immunoprecipitation with Hif-1α antibody and Western blotting with ubiquitin antibody to detect ubiquitinated Hif-1α in both wild type and *UCHL1−/−* hiPSC-CMs. In addition, MG132 was added to inhibit proteasomal protein degradation (Fig. 3F). As shown in Fig. 3G, knockout of UCHL1 significantly enhanced ubiquitination of HIF-1α and treatment of MG132 normalized the difference of ubiquitinated HIF-1α between wild type and *UCHL1−/−* hiPSC-CMs. These results strongly suggested that UCHL1 may serve as deubiquitination enzyme to stabilize Hif-1α.

3.4. UCHL1 controls nuclear translocation of HIF-1α

In addition to stabilizing HIF-1α, an interesting observation was made with immunoflourescent staining. As shown in Fig. 4A, while HIF-1α could enter nucleus in wild type hiPSC-CM after hypoxia treatment, majority of HIF-1α was still in cytosol in hypoxia treated *UCHL1−/−* hiPSC-CM. Furthermore, cell fractionation experiments also showed that UCHL1 localized to nuclear fraction in hypoxia condition (Supplemental Fig. S3). Since Hif-1α is a transcriptional factor, we performed real-time RT-PCR to quantify its target genes in both wild type and *UCHL−/−* hiPSC-CMs. Consistent with immunostaining results, while HIF-1α target genes upregulated upon hypoxia treatment, the level of these genes were significantly higher in wild type hiPSCs-CM than those in *UCHL1−/−* hiSPC-CM in both normoxia and hypoxia conditions. Taken together, our studies suggested that UCHL1 could control both stability and localization of HIF-1α, in turn to regulate HIF-1α mediated cardioprotection.

3.5. UCHL1 might be a therapeutic target to treat myocardial infarction

To test the potential translational application of UCHL1, we purified recombinant human UCHL1 (rhUCHL1) protein from *E. Coli* expression system. Coomassie blue staining was used to confirm the purity of rhUCHL1 (Supplemental Fig. S4). Purified UCHL1 protein was delivered to mouse via intraperitoneal (IP) injection before and after MI surgery (8 mg/kg/day) (Fig. 5A). Echocardiogram analysis showed that the ejection fraction of rhUCHL1 injected group was higher than that of control group at 14 day after MI surgery (Fig. 5B and C). Since rhUCHL1 was systemically administrated, we further tested specifically upregulating UCHL1 in cardiomyocytes. To test this hypothesis, adeno-associated virus (AAV9-cTNT-m-Uchl1-WPRE) was used to express UCHL1. We used AAV9, because previous studies showed that AAV9 is the serotype that infect heart with higher efficiency. Furthermore, UCHL1 expression is driven by cTNT promoter, which further enhanced tissue specificity of AAV mediated UCHL1 delivery. Eight weeks after

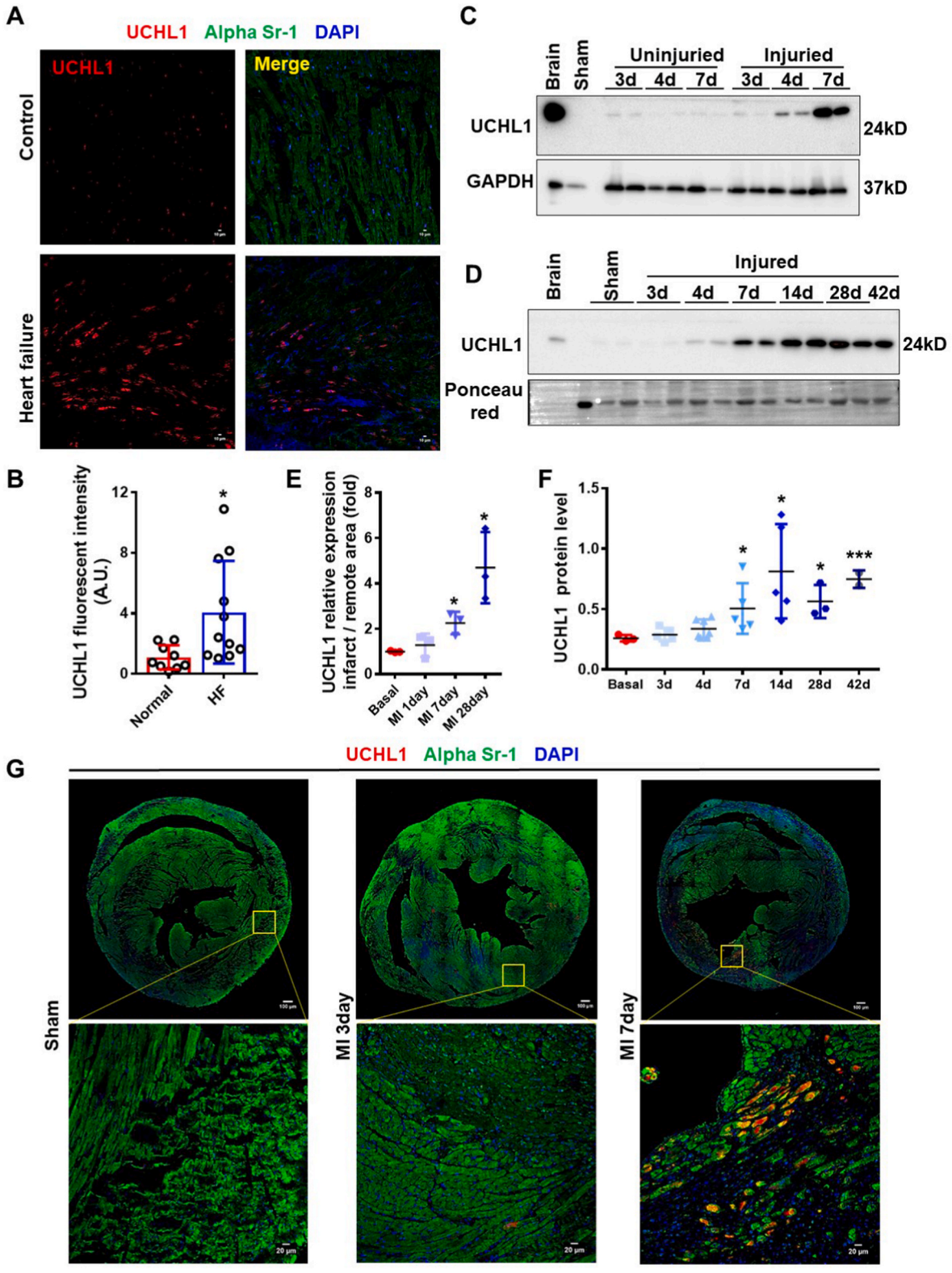

Fig. 1. UCHL1 is upregulated in both human heart failure samples and murine myocardial infarction model. (A) Frozen human heart sections were immunohistochemically stained with UCHL1 antibody. **(B)** Quantification of UCHL1 expression in frozen human heart sections. **(C)** Western blotting (WB) analysis shows UCHL1 upregulation in infarct zone of mouse hearts, but not in the remote zone after MI surgery. **(D)** WB analysis for UCHL1 at different time pionts (3, 4, 7, 14, 28, 42 days) in infarct zone of mouse hearts after MI surgery. **(E)** Real-time RT-PCR analysis of UCHL1 mRNA levels in infarct heart tissues. **(F)** The quantitative densitometric analysis of UCHL1 protein level showing in panel **D**. **(G)** Immunofluorescence detection of UCHL1 in mouse hearts, UCHL1 immunofluorescence is rendered in red and α-sarcomeric actin (Alpha Sr-1) immunofluorescence in green (*P < 0.05, **P < 0.01, ***P < 0.001). (For interpretation of the references to color in this figure legend, the reader is referred to the Web version of this article.)

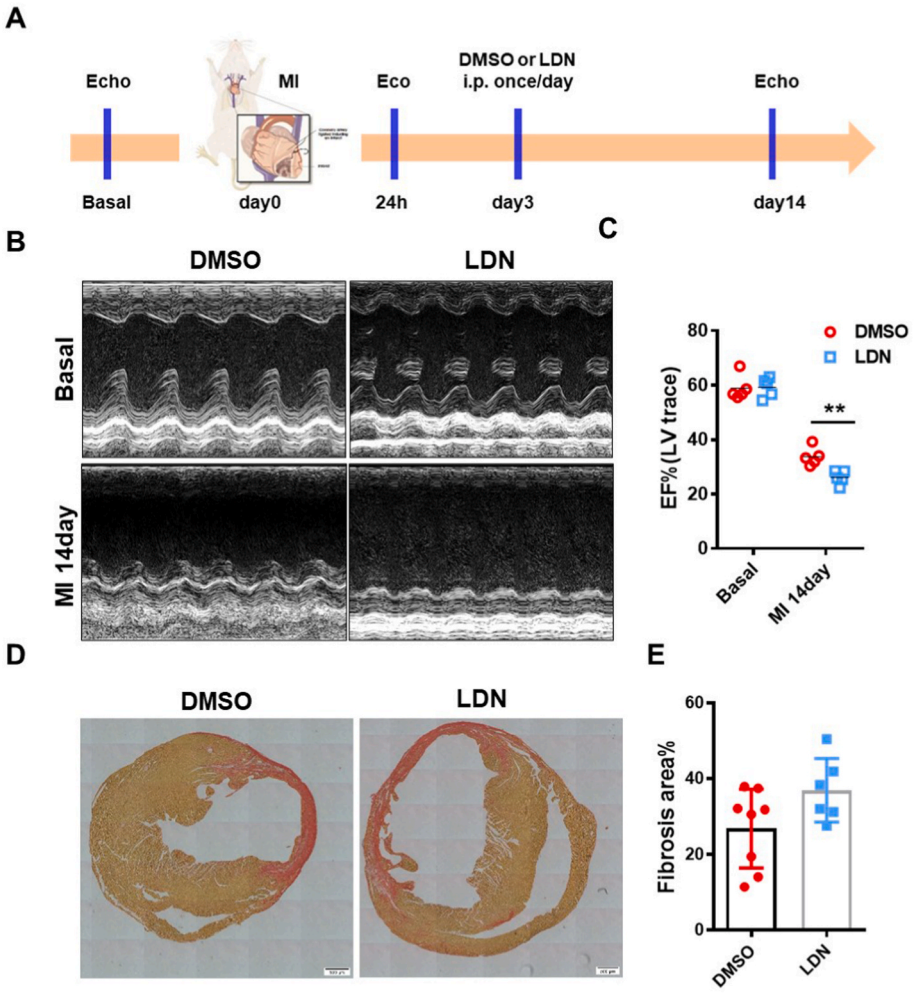

Fig. 2. Pharmacological inhibition of UCHL1 compromises cardiac function following MI. (A) The flow chart demonstrates the administration of LDN57444 to MI injured mice. **(B)** Representative images of M-mode echocardiography in different groups. **(C)** Quantification of ejection fraction (EF) after echocardiography of mice. **(D)** Representative images of Sirius Red staining of heart tissues. **(E)** Quantification analysis of fibrosis area in mouse hearts. (**P < 0.01). (For interpretation of the references to color in this figure legend, the reader is referred to the Web version of this article.)

AAV injection, MI surgery was performed to UCHL1 overexpression and control mice. Similar to systemic administration of rhUCHL1, AAV mediated cardiomyocyte specific overexpression of UCHL1 could also protect hearts against MI induced cardiac dysfunction as shown by echocardiogram (Fig. 5D, E, and 5F). Thus, UCHL1 might serve as a potential target to treat myocardial infarction induced injury.

4. Discussion

In this study, we used both mouse MI model and hiPS-CM to reveal a novel role for UCHL1 in cardiac protection. Immunofluorescent staining shows UCHL1 specifically up-regulated in cardiomyocytes after MI surgery and failing human hearts. Pharmacological inhibition of UCHL1 exacerbated the heart function after MI, suggesting a protective role of UCHL1 after MI. Mechanistically, proximity-labeling assay revealed HIF-1α as the potential target of UCHL1 in hypoxic cardiomyocytes. Finally, this study suggested UCHL1 might be a potential therapeutic target for treating myocardial infarction.

UCHL1 was commonly recognized as a neuronal marker [24]. Similar to ubiquitin, UCHL1 is a component of cellular aggregates that are indicative of neurodegenerative disease such as Lewy bodies in Parkinson's disease (PD) [25]. Dobaczewski et al. for the first time, found that UCHL1 was dramatically elevated in cardiomyocytes at day 7 after MI and lasted for at least 21 days, however, the underlying mechanism was largely unclear [26]. Recently, researchers found UCHL1 was up-regulated in cardiac fibroblasts after MI [17], raising the question that which is the primary cell type that overexpresses UCHL1 in response to MI. Our data presented in this study indicated cardiomyocytes, rather than cardiac fibroblasts, might be the source of UCHL1 after MI injury (Fig. 1A and **G**). We also had direct observation that UCHL1 was increased in hiPS-CM after hypoxia treatment (Fig. 3C and **E**). When we treated cardiac fibroblasts with hypoxia, we failed to observe upregulation of UCHL1 (data not shown). In addition, other researchers also found UCHL1 was cardiomyocytes of hypertrophic failing hearts [16]. In their study, the administration of LDN-57444 was sufficient and effective to reverse cardiac hypertrophy and dysfunction after hypertrophic stimuli. On the contrary, our results indicated that LDN-57444 mediated UCHL1 inhibition could exacerbate heart function after MI as compared to control group (Fig. 2B and C). Although there is no statistical difference in cardiac fibrosis between LDN-57444 treated and control hearts, there is a slight trend indicating LDN-57444 treatment might increase cardiac fibrosis after MI (Fig. 2D and E). This further suggested that the primary target of UCHL1 overexpression might be cardiomyocytes rather than cardiac fibroblasts.

Another important finding of our study was that UCHL1 interacted with HIF-1α in cardiomyocyte under hypoxia condition (Fig. 3). Although UCHL1-HIF-1α axis has already been reported in cancer cell radioresistance and tumor cell migration [21–23], there was no study to investigate the function of this signaling pathway in cardiovascular physiology and diseases. As redox induced injury plays an important role in MI injury and HIF-1α could protect cardiomyocytes by inducing a range of cardioprotective genes that allow the cells to survive in the hypoxic environment [27], studies reveal molecular and cellular mechanisms of HIF-1α signaling could be potentially important. In our study, we used a proximity-labeling system, which allowed us to study the potential interacting patterners of UCHL1 in live cells under hypoxia

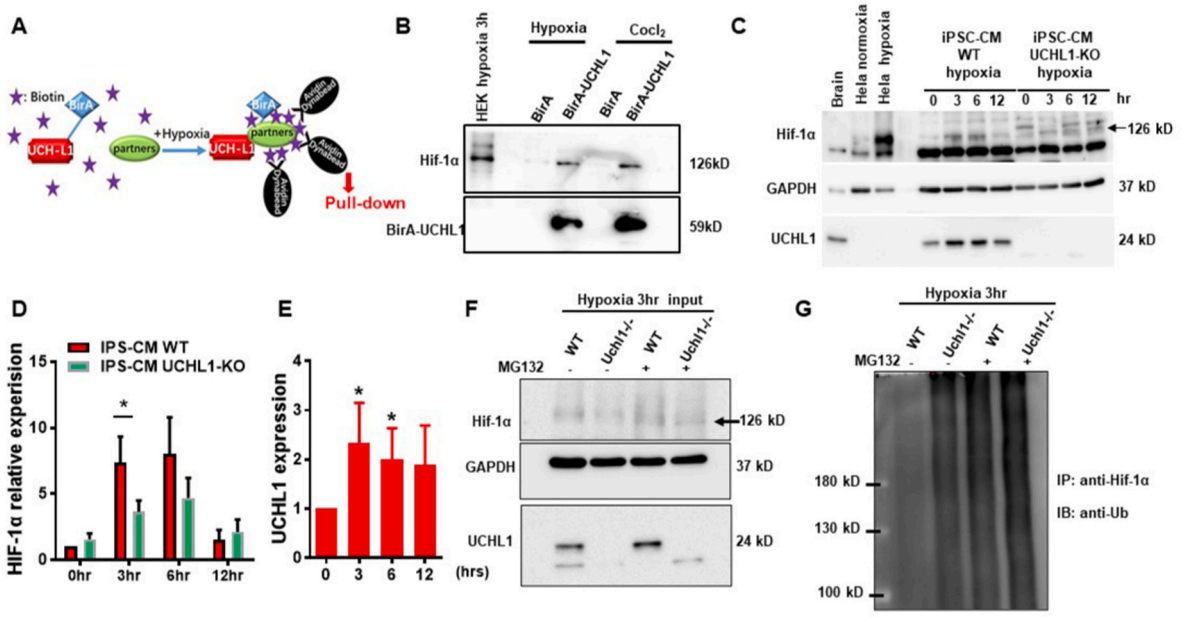

Fig. 3. HIF-1α is a potential target of UCHL1 after myocardial infarction (MI). (A) Schematic representation of UCHL1 proximity-labeling by BioID. In the presence of biotin, the BirA-UCHL1 fusion protein biotinylates nearby proteins which can be affinity captured through streptavidin magnetic beads. **(B)** WB analysis of affinity captured material from BioID assay using cell lysates from HEK293T cells treated with hypoxia or $CoCl_2$. **(C)** WT and *UCHL1*−/− hiPSC-CM cells were treated with hypoxia for 0, 3, 6, 12 h, and the levels of HIF-1α and UCHL1 protein were analyzed by WB. **(D)** Quantification results from three independent WB of HIF-1α in panel **D**. **(E)** Quantification results from three independent western blots of UCHL1 in panel **D**. **(F)** Representative WB analysis of WT and *UCHL1*−/− hiPSC-CMs treated hypoxia with or without MG132. **(G)** Ubiquitination of HIF-1α was examined by immunoprecipitation (IP) analysis. The anti–HIF–1α antibody was used for IP, and ubiquitinated HIF-1α was detected by anti-ubiquitin antibody (*P < 0.05).

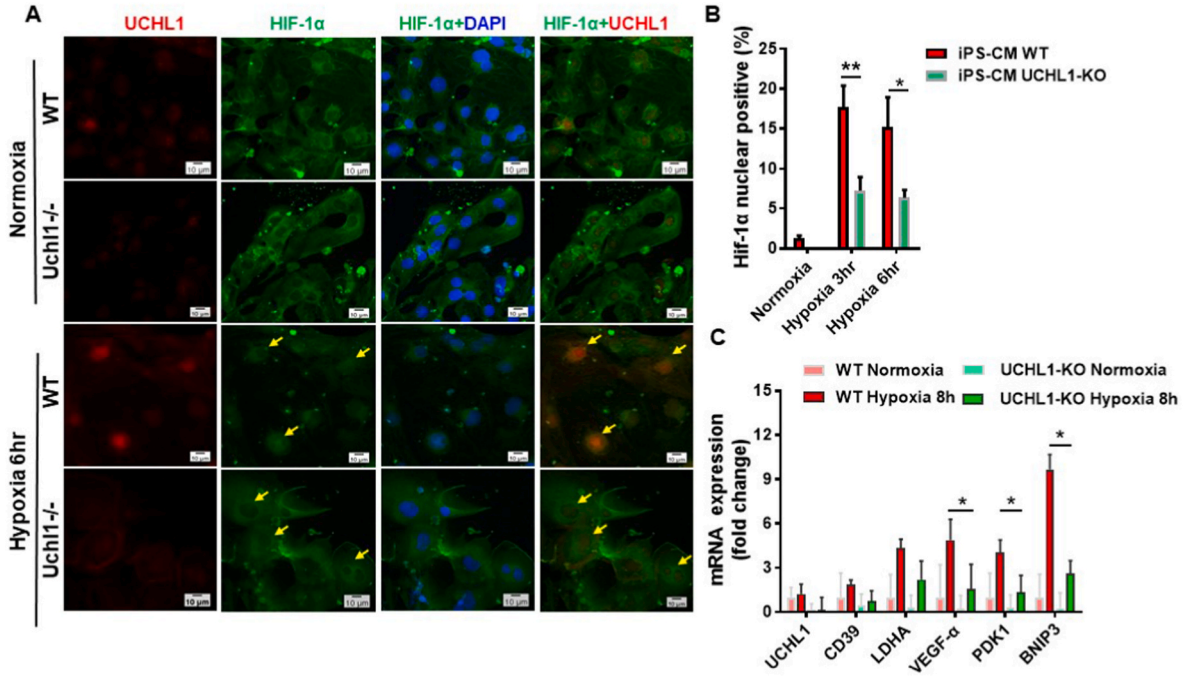

Fig. 4. UCHL1 controls nuclear translocation of HIF-1α. (A) hiPSC-CMs were subjected to Immunofluorescence staining of UCHL1 (red) and HIF-1α (green) in normoxic and hypoxic conditions. **(B)** Quantitation of HIF-1α influx in nuclei in WT and *UCHL1*−/− hiPSC-CMs in normoxic and hypoxic conditions. **(C)** Real time RT-PCR was performed to measure mRNA levels of UCHL1, HIF-1α target genes (CD39, LDHA, VEGF-α, PDK1 and BNIP3) in WT and *UCHL1*−/− hiPSC-CMs under normoxic and hypoxic conditions. (*P < 0.05, **P < 0.01, ***P < 0.001). (For interpretation of the references to color in this figure legend, the reader is referred to the Web version of this article.)

condition (Fig. 3A). Consistent to previous studies, HIF-1α was identified as a potential target interacting with UCHL1(Fig. 3B). The underlying mechanism of UCHL1 cardiac protection may be due to HIF-1α stabilization (Fig. 3C, D, and 3G). More interestingly, we also observed UCHL1 might control nuclear translocation of HIF-1α upon hypoxia (Fig. 4A), although the detailed mechanisms remain to be elucidated.

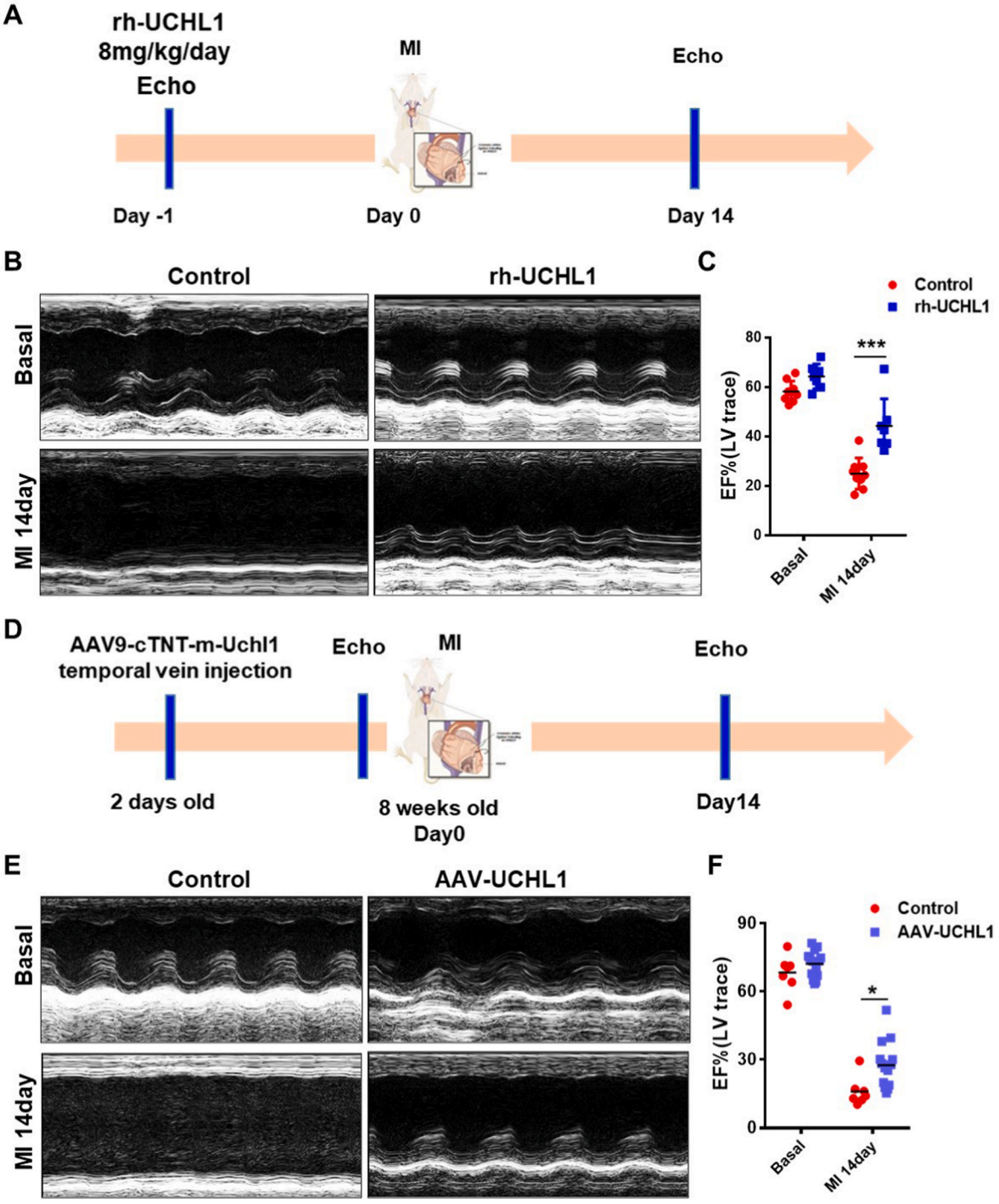

Fig. 5. UCHL1 might be a therapeutic target to treat MI. (A) The flow chart of administration of rhUCHL1 to treat mice after MI surgery. **(B)** Representative images of M-mode echocardiography in different groups. **(C)** Quantification of ejection fraction (EF) after echocardiography of mice. **(D)** The flow chart of studying the role of AAV mediated cardiac specific delivery of UCHL1 in MI injured mice. **(E)** Representative images of M-mode echocardiography in different groups. **(F)** Quantification of ejection fraction (EF) after echocardiography of mice (*$P < 0.05$, **$P < 0.01$, ***$P < 0.001$).

Hypoxia has also been found to play a role in promoting the proliferation of a variety of mammalian cell types such as embryonic stem cells [28], smooth muscle cells [29] and endothelial cells [30]. Furthermore, in adult zebrafish, exposure to chronic hypoxia leads to an increased number of cardiomyocytes [31]. Hypoxia treatment could also induce heart regeneration in adult mice and the potential target could be HIF-1α [32]. In our study, UCHL1 positive cardiomyocytes were identified in the border zone of infarct and non-infarct mouse hearts (Fig. 1G and Supplemental Fig. S1). Furthermore, we have performed immunostaining of BrdU (proliferating cell marker), Alpha Sr-1 (cardiomycyte marker), and UCHL1 (Supplemental Fig. S5). We did identify some cells were triple positive for all of markers. Given the upregulation of UCHL1 was observed 3 days after MI injury, this might suggest UCHL1-HIF-1α signaling axis might promote cardiomyocytes proliferation/regeneration after MI, which is one of key direction of our further research.

Of course, there are still some questions need to be addressed. For example, what are the upstream factors that control upregulation of

UCHL1 following MI? To address this question, we have performed some RNA sequencing with samples from health left ventricle and infarct hearts. We hope to identify potential factors that could regulate expression of UCHL1 by analyzing the RNA seq data. In addition, published study also suggested that UCHL1 might contribute to cardiac hypertrophy and fibrosis [16]. While our data implied that UCHL1 inhibition might enhance cardiac fibrosis following MI injury (Fig. 2D), more studies will be required to dissect the detailed function of UCHL1 in cardiac fibrosis.

In summary, our study demonstrates that UCHL1 could preserve heart function after MI by interacting with and stabilizing HIF1α. Interventions that target the UCHL1-HIF1α interaction may be a potential therapeutic strategy to treat MI.

Author contributions

H.Z., B.G. and X.W. designed the research. B.G., X.W., K.H.P., K.E.L., J.K., P.C., X.Z., T.T., C.Y., X.Z. and C.C. performed research and data analyses. P.M.J, L.C., and L. Y. provided valuable suggestions to the study. H.Z. and B.G. wrote the manuscript.

Declaration of competing interest

The authors declare no conflict of interests.

Acknowledgements

This work was supported by NIH grants (AR067766, EY030621 and HL153876) and AHA grant (19TPA34850169) to H.Z. We thank the patients and investigators who participated in the Lifeline of Ohio Organ Procurement Program (LOOP) for providing the specimens and clinical data.

Appendix A. Supplementary data

Supplementary data to this article can be found online at https://doi.org/10.1016/j.redox.2022.102295.

References

[1] J.S. Lawton, J.E. Tamis-Holland, S. Bangalore, E.R. Bates, T.M. Beckie, J. M. Bischoff, J.A. Bittl, M.G. Cohen, J.M. DiMaio, C.W. Don, S.E. Fremes, M. F. Gaudino, Z.D. Goldberger, M.C. Grant, J.B. Jaswal, P.A. Kurlansky, R. Mehran, T. S. Metkus Jr., L.C. Nnacheta, S.V. Rao, F.W. Sellke, G. Sharma, C.M. Yong, B. A. Zwischenberger, ACC/AHA/SCAI guideline for coronary artery revascularization: executive summary: a report of the American college of cardiology/American heart association joint committee on clinical practice guidelines, Circulation 145 (2021) e4–e17, 2022.

[2] M. Writing Committee, J.S. Lawton, J.E. Tamis-Holland, S. Bangalore, E.R. Bates, T.M. Beckie, J.M. Bischoff, J.A. Bittl, M.G. Cohen, J.M. DiMaio, C.W. Don, S. E. Fremes, M.F. Gaudino, Z.D. Goldberger, M.C. Grant, J.B. Jaswal, P.A. Kurlansky, R. Mehran, T.S. Metkus Jr., L.C. Nnacheta, S.V. Rao, F.W. Sellke, G. Sharma, C. M. Yong, B.A. Zwischenberger, ACC/AHA/SCAI guideline for coronary artery revascularization: executive summary: a report of the American college of cardiology/American heart association joint committee on clinical practice guidelines, J. Am. Coll. Cardiol. 79 (2021) 197–215, 2022.

[3] L.M. Buja, D. Vela, Cardiomyocyte death and renewal in the normal and diseased heart, Cardiovasc. Pathol. 17 (2008) 349–374.

[4] S.H. Lee, P.L. Wolf, R. Escudero, R. Deutsch, S.W. Jamieson, P.A. Thistlethwaite, Early expression of angiogenesis factors in acute myocardial ischemia and infarction, N. Engl. J. Med. 342 (2000) 626–633.

[5] S.G. Ong, D.J. Hausenloy, Hypoxia-inducible factor as a therapeutic target for cardioprotection, Pharmacol. Ther. 136 (2012) 69–81.

[6] G.L. Wang, B.H. Jiang, E.A. Rue, G.L. Semenza, Hypoxia-inducible factor 1 is a basic-helix-loop-helix-PAS heterodimer regulated by cellular O2 tension, Proc. Natl. Acad. Sci. U. S. A. 92 (1995) 5510–5514.

[7] J. Gunter, A. Ruiz-Serrano, C. Pickel, R.H. Wenger, C.C. Scholz, The functional interplay between the HIF pathway and the ubiquitin system - more than a one-way road, Exp. Cell Res. 356 (2017) 152–159.

[8] S. Jain, E. Maltepe, M.M. Lu, C. Simon, C.A. Bradfield, Expression of ARNT, ARNT2, HIF1 alpha, HIF2 alpha and Ah receptor mRNAs in the developing mouse, Mech. Dev. 73 (1998) 117–123.

[9] M. Kido, L. Du, C.C. Sullivan, X. Li, R. Deutsch, S.W. Jamieson, P.A. Thistlethwaite, Hypoxia-inducible factor 1-alpha reduces infarction and attenuates progression of cardiac dysfunction after myocardial infarction in the mouse, J. Am. Coll. Cardiol. 46 (2005) 2116–2124.

[10] J.E. Rodriguez, J.C. Schisler, C. Patterson, M.S. Willis, Seek and destroy: the ubiquitin——proteasome system in cardiac disease, Curr. Hypertens. Rep. 11 (2009) 396–405.

[11] H. Su, X. Wang, The ubiquitin-proteasome system in cardiac proteinopathy: a quality control perspective, Cardiovasc. Res. 85 (2010) 253–262.

[12] C. Hu, Y. Tian, H. Xu, B. Pan, E.M. Terpstra, P. Wu, H. Wang, F. Li, J. Liu, X. Wang, Inadequate ubiquitination-proteasome coupling contributes to myocardial ischemia-reperfusion injury, J. Clin. Invest. 128 (2018) 5294–5306.

[13] D.N. Suong, D.T. Thao, Y. Masamitsu, T.L. Thuoc, Ubiquitin carboxyl hydrolase L1 significance for human diseases, Protein Pept. Lett. 21 (2014) 624–630.

[14] P. Bishop, D. Rocca, J.M. Henley, Ubiquitin C-terminal hydrolase L1 (UCH-L1): structure, distribution and roles in brain function and dysfunction, Biochem. J. 473 (2016) 2453–2462.

[15] Y. Luo, J. He, C. Yang, M. Orange, X. Ren, N. Blair, T. Tan, J.M. Yang, H. Zhu, UCH-L1 promotes invasion of breast cancer cells through activating Akt signaling pathway, J. Cell. Biochem. 119 (2018) 691–700.

[16] H.L. Bi, X.L. Zhang, Y.L. Zhang, X. Xie, Y.L. Xia, J. Du, H.H. Li, The deubiquitinase UCHL1 regulates cardiac hypertrophy by stabilizing epidermal growth factor receptor, Sci. Adv. 6 (2020), eaax4826.

[17] Q. Lei, T. Yi, H. Li, Z. Yan, Z. Lv, G. Li, Y. Wang, Ubiquitin C-terminal hydrolase L1 (UCHL1) regulates post-myocardial infarction cardiac fibrosis through glucose-regulated protein of 78 kDa (GRP78), Sci. Rep. 10 (2020) 10604.

[18] B.C. Geng, K.H. Choi, S.Z. Wang, P. Chen, X.D. Pan, N.G. Dong, J.K. Ko, H. Zhu, A simple, quick, and efficient CRISPR/Cas9 genome editing method for human induced pluripotent stem cells, Acta Pharmacol. Sin. 41 (2020) 1427–1432.

[19] M.T. Zhao, H. Chen, Q. Liu, N.Y. Shao, N. Sayed, H.T. Wo, J.Z. Zhang, S.G. Ong, C. Liu, Y. Kim, H. Yang, T. Chour, H. Ma, N.M. Gutierrez, I. Karakikes, S. Mitalipov, M.P. Snyder, J.C. Wu, Molecular and functional resemblance of differentiated cells derived from isogenic human iPSCs and SCNT-derived ESCs, Proc. Natl. Acad. Sci. U. S. A. 114 (2017) E11111–E11120.

[20] L. Ye, G. D'Agostino, S.J. Loo, C.X. Wang, L.P. Su, S.H. Tan, G.Z. Tee, C.J. Pua, E. M. Pena, R.B. Cheng, W.C. Chen, D. Abdurrachim, J. Lalic, R.S. Tan, T.H. Lee, J. Zhang, S.A. Cook, Early regenerative capacity in the porcine heart, Circulation 138 (2018) 2798–2808.

[21] R. Nakashima, Y. Goto, S. Koyasu, M. Kobayashi, A. Morinibu, M. Yoshimura, M. Hiraoka, E.M. Hammond, H. Harada, UCHL1-HIF-1 axis-mediated antioxidant property of cancer cells as a therapeutic target for radiosensitization, Sci. Rep. 7 (2017) 6879.

[22] X. Li, A. Hattori, S. Takahashi, Y. Goto, H. Harada, H. Kakeya, Ubiquitin carboxyl-terminal hydrolase L1 promotes hypoxia-inducible factor 1-dependent tumor cell malignancy in spheroid models, Cancer Sci 111 (2020) 239–252.

[23] Y. Goto, L. Zeng, C.J. Yeom, Y. Zhu, A. Morinibu, K. Shinomiya, M. Kobayashi, K. Hirota, S. Itasaka, M. Yoshimura, K. Tanimoto, M. Torii, T. Sowa, T. Menju, M. Sonobe, H. Kakeya, M. Toi, H. Date, E.M. Hammond, M. Hiraoka, H. Harada, UCHL1 provides diagnostic and antimetastatic strategies due to its deubiquitinating effect on HIF-1alpha, Nat. Commun. 6 (2015) 6153.

[24] K.D. Wilkinson, K.M. Lee, S. Deshpande, P. Duerksen-Hughes, J.M. Boss, J. Pohl, The neuron-specific protein PGP 9.5 is a ubiquitin carboxyl-terminal hydrolase, Science 246 (1989) 670–673.

[25] J. Lowe, H. McDermott, M. Landon, R.J. Mayer, K.D. Wilkinson, Ubiquitin carboxyl-terminal hydrolase (PGP 9.5) is selectively present in ubiquitinated inclusion bodies characteristic of human neurodegenerative diseases, J. Pathol. 161 (1990) 153–160.

[26] A. Drobysheva, M. Ahmad, R. White, H.W. Wang, F.H. Leenen, Cardiac sympathetic innervation and PGP9.5 expression by cardiomyocytes after myocardial infarction: effects of central MR blockade, Am. J. Physiol. Heart Circ. Physiol. 305 (2013) H1817–H1829.

[27] C.X. Santos, N. Anilkumar, M. Zhang, A.C. Brewer, A.M. Shah, Redox signaling in cardiac myocytes, Free Radic. Biol. Med. 50 (2011) 777–793.

[28] C.E. Forristal, K.L. Wright, N.A. Hanley, R.O. Oreffo, F.D. Houghton, Hypoxia inducible factors regulate pluripotency and proliferation in human embryonic stem cells cultured at reduced oxygen tensions, Reproduction 139 (2010) 85–97.

[29] A. Cogo, G. Napolitano, M.C. Michoud, D.R. Barbon, M. Ward, J.G. Martin, Effects of hypoxia on rat airway smooth muscle cell proliferation, J. Appl. Physiol. 94 (1985) 1403–1409, 2003.

[30] W. Li, M. Petrimpol, K.D. Molle, M.N. Hall, E.J. Battegay, R. Humar, Hypoxia-induced endothelial proliferation requires both mTORC1 and mTORC2, Circ. Res. 100 (2007) 79–87.

[31] C. Jopling, G. Sune, A. Faucherre, C. Fabregat, J.C. Izpisua Belmonte, Hypoxia induces myocardial regeneration in zebrafish, Circulation 126 (2012) 3017–3027.

[32] Y. Nakada, D.C. Canseco, S. Thet, S. Abdisalaam, A. Asaithamby, C.X. Santos, A. M. Shah, H. Zhang, J.E. Faber, M.T. Kinter, L.I. Szweda, C. Xing, Z. Hu, R. J. Deberardinis, G. Schiattarella, J.A. Hill, O. Oz, Z. Lu, C.C. Zhang, W. Kimura, H. A. Sadek, Hypoxia induces heart regeneration in adult mice, Nature 541 (2017) 222–227.